Supporting Information

The Study on Defect-rich Carbon-Spheres as Metal-Free Electrocatalyst for Efficient Oxygen Reduction Reaction

Qin Xiang, Wei Yin, Yuping Liu, Danmei Yu, Xiaoli Wang, Sha Li, Changguo Chen*

College of Chemistry and Chemical Engineering, Chongqing University, Chongqing 401331, China.

Materials. All chemicals used were analytical grade and not further purification.

Preparation of CSs-t. A given amount of iron trichloride hexahydrate (FeCl$_3$ 6H$_2$O) and iodine (I$_2$) were dissolved in ethanol, the mole ratios of iron to iodine are 16:1, 32:1, 38:1, 46:1, respectively. Take the molar ratio 16:1 as an example, 4.8 g FeCl$_3$ 6H$_2$O and 0.28 g I$_2$ were dissolved in 25 mL ethanol. Samples of other molar ratios can be obtained in a similar way with different quality of FeCl$_3$ 6H$_2$O (9.4g, 11.2g and 13.7g, respectively), the amount of I$_2$ was kept constant at 0.28 g. The reddish brown solution obtained was transferred into a 50 ml Teflon autoclave, which was heated to 160℃ and kept at this temperature for 20 h. After cooling to room temperature naturally, black powder was obtained, which was subsequently washed with 1M HCl and then with water and ethanol several times to remove the residual iron and iodine. Then, the resulting sample was treated by refluxing in 1 M H$_2$SO$_4$ aqueous solution at 90℃ for 4 h, then washed and dried overnight at 80 ℃. The sample is denoted as CSs-20h. As control samples, the other CSs-t (t = 16, 24, and 28h) were synthesized in the same manner, but at a different solvothermal time (16, 24, and 28h, respectively).

Preparation of CSs-t-900. CSs-t products were then calcined at 900 ℃ for 1 h in a vacuum atmosphere to form CSs-t-900 (t = 16, 20, 24 and 28h, respectively). These catalysts can be reproduced easily.

Characterization. The morphology and chemical composition of samples were investigated by FESEM (JSM-7800F), XPS (ESCALAB250Xi), FTIR (Nicolet 550II)

and TGA (Shimadzu DTG-60H). The phase composition and crystallinity of samples were investigated by XRD (Shimadzu XRD6000) and Raman (LabRAM HR Evolution). Specific surface areas and pore size distributions were determined from nitrogen sorption isotherms collected at 77 K on Quadrasorb 2MP apparatus.

Electrochemical measurements. The working electrode was prepared as follows: 5 mg of the CSs-t-900 was dispersed in 625 μL solvent mixture of 450 μL of water, 50 μL of ethanol, and 125 μL of 5 wt.% Nafion solution, under sonication for 1 h to form a homogeneous ink. Then 10 μL of the resulting catalyst ink was dropped onto a pre-polished rotating disk electrode (RDE, $\Phi = 5$ mm, the loading of the catalysts was 0.407 mg cm^{-2}) and allowed to dry in air naturally. For comparison, a 20 wt.% JM-Pt/C at loadings of 0.13 mg cm^{-2}, and electrode preparation was same as the used for CSs-t-900. Electrochemical measurements were performed on an electrochemical workstation (CHI760E, CH Instrument, China) equipped with a conventional three-electrode electrochemical cell, and controlled at 25℃ using a water-bath. The counter electrode was Pt wire, and the reference electrode was an Ag/AgCl. All potentials were later converted to the reversible hydrogen electrode (RHE) scale, the calibration was performed in the high-purity H$_2$ saturated electrolyte with Pt wires as the working and counter electrodes. The ORR was carried out in an N$_2$- or O$_2$-saturated 150 ml 0.1 M KOH, including cyclic voltammetry (CV), linear sweep voltammetry (LSV) and chronoamperometric response $i–t$. For the RDE measurements, the scan rate was 10 mV s^{-1} and the disk rotation rate was from 400 to 2500 rpm. Afterwards, the durability of the catalyst was tested by running given number of cycles in O$_2$ atmosphere using the potential sweep from 0.6 V to 0.9 V (vs. RHE) at 50 mV s^{-1}. Methanol (5 mL) was added to the O$_2$ saturated 0.1 M KOH solution around 400 s and 700 s, respectively, for the durability test. The current was recorded at 0.4 V vs. RHE with 1600 rpm.

Calculation of the kinetic-limiting current (j_k) and the electron transfer number (n).

According to the Koutecky-Levich equation given below:

$$j^{-1}=j_k^{-1}+B^{-1}\omega^{-1/2}$$

Where j is the measured current, ω donates the rotation speed in rpm, and B, the reciprocal of the slope, could be determined from the slope of Koutecky-Levich plots based on Levich equation as follows:

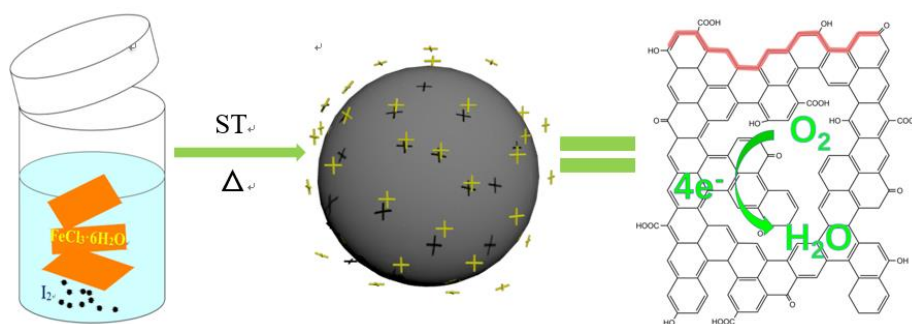$$B = 0.2nFC_{O2}\,(D_{O2})^{2/3}v^{-1/6}$$

F: The Faraday constant (96,485 C mol^{-1});

C_{O2}: The bulk concentration of O_2 (1.2×10^{-6} mol cm^{-3});

D_{O2}: The diffusion coefficient of O_2 in 0.1 M KOH (1.9×10^{-5} cm^2 s^{-1});

v: The kinetic viscosity (0.01 cm^2 s^{-1}).

The constant 0.2 is adopted when the rotation speed is expressed in rpm.

Schematic illustration for defect-rich structure of carbon-spheres

Solvothermal carbonization of ethanol can produce numbers of CSs with rich-edges and porous structure on the surface, and the incomplete oxidation and carbonization leaving residual O-containing species on the surfaces of the CSs, the incorporation of O-containing functional groups with a higher electronegativity, generates positive charge density on the adjacent carbon atoms. Additionally, the numbers of intercalated H_2O or H^+ was removed through sequential dehydration gave rise to abundant dangling bonds located at the edge of sp^2 carbon. Both are favorable for the chemisorption of O_2, decreasing the overpotential, and leading to a faster kinetics, is beneficial to an efficient 4 e^- process for ORR.
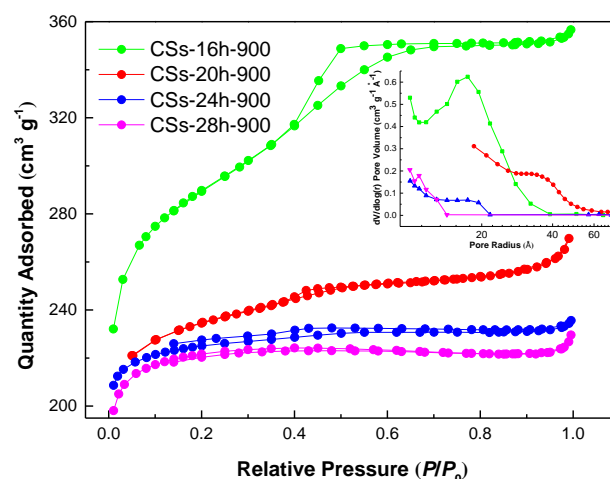

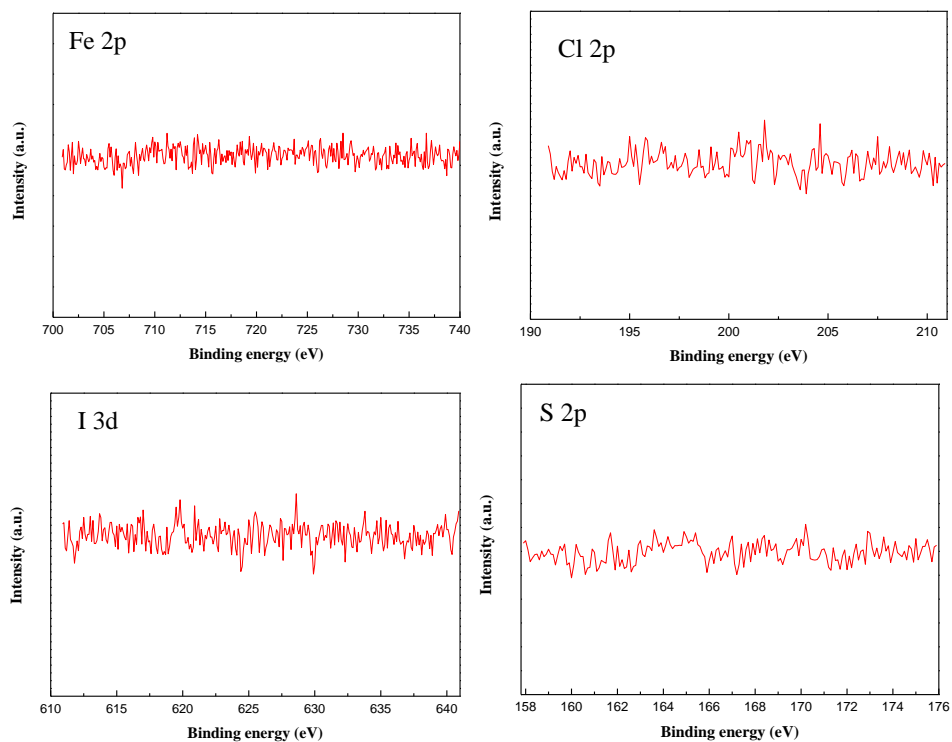**Figure S1.** N_2 adsorption/desorption isotherms of all CSs-t-900.

Figure S2. High resolution XPS: Fe 2p(A), Cl 2p(B), I 3d(C), and S 2p(D) of CSs-20h-900.
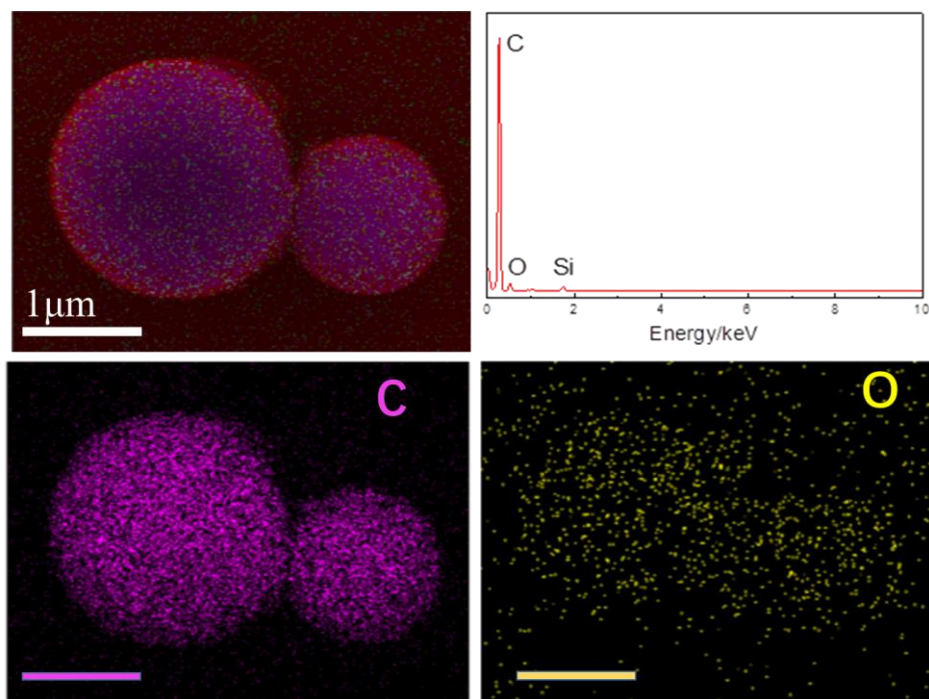

Figure S3. FESEM image of CSs-20h-900, and the corresponding mapping images of C and O.
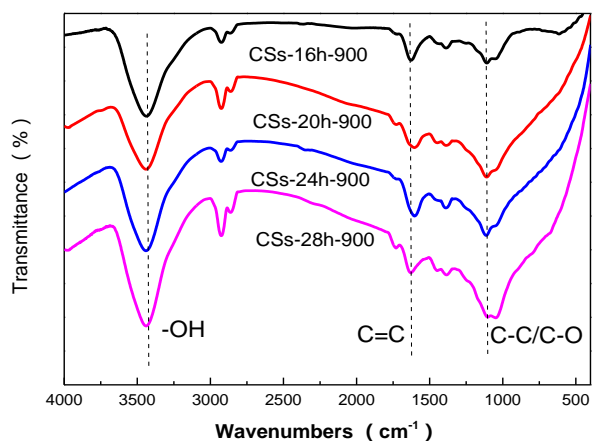
Figure S4. FTIR spectra of CSs-t-900 prepared with different solvothermal reaction time of 16, 20, 24, and 28h.

In the FTIR spectrum of CSs-t-900, peaks near 1110 cm⁻¹ are corresponding to the vibration modes of C-O and C-C groups, near 1640 cm⁻¹ are assigned to C=C vibrations, which results from the dehydration, peaks at 2850-2960 cm⁻¹ belong to C-H vibrations, and peaks near 3400 cm⁻¹ attributed to O-H vibrations. The increase of 1110 and 3400 cm⁻¹ with ST indicating the further carbonization and aromatization of ethanol.
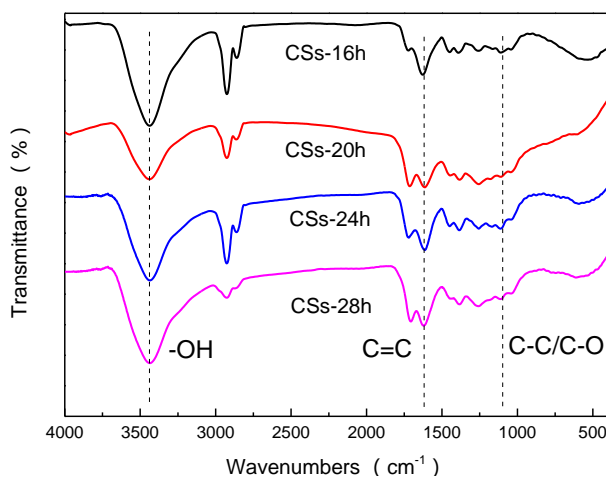

Figure S5. FTIR spectra of CSs-t prepared with different solvothermal reaction time of 16, 20, 24, and 28h.

In the FTIR spectra, typical peaks belonging to CSs-t-900 (Figure 2D) were observed in all samples, but with a decreased intensity, indicating the further carbonization caused by high temperature pyrolysis. Especially the peak near 1110 cm⁻¹ which results from the vibration modes of C-O and C-C groups[3e].
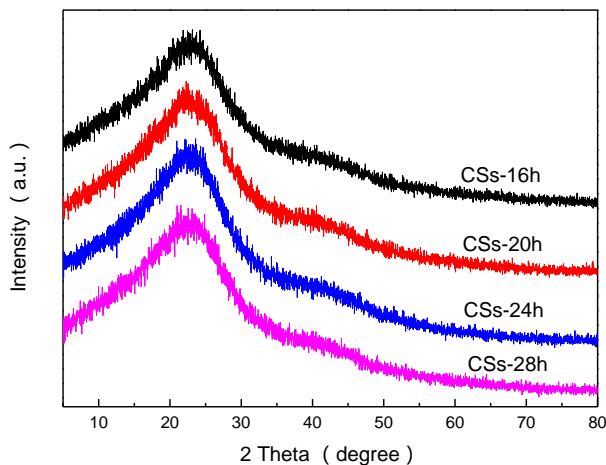
Figure S6. XRD pattern of pristine carbon spheres prepared with different solvothermal reaction time of 16, 20, 24, and 28h.

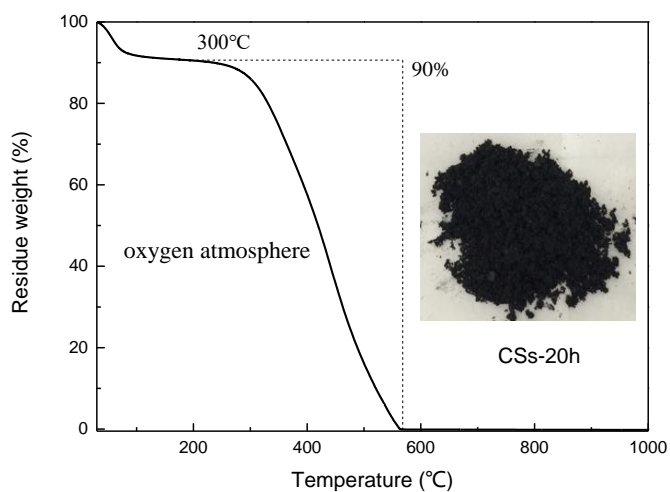Only one broad peak near 24°, attributed to highly disordered and ungraphitized carbon structures.

Figure S7. TGA of CSs-20h in O_2 with a temperature rise rate of 10 ℃ min^{-1}.

The curve fall down (10%) prior to 100 ℃ was due to the moisture loss, and the weight loss (90%) after 300 ℃ may ascribe to the carbon oxidized by O_2, the ratio of the weight of residual and starting materials approaches zero at about 570 ℃, which are nearly the same with the data for pure carbon materials reported in the literature[1], revealing that there is no metal present in the sample.
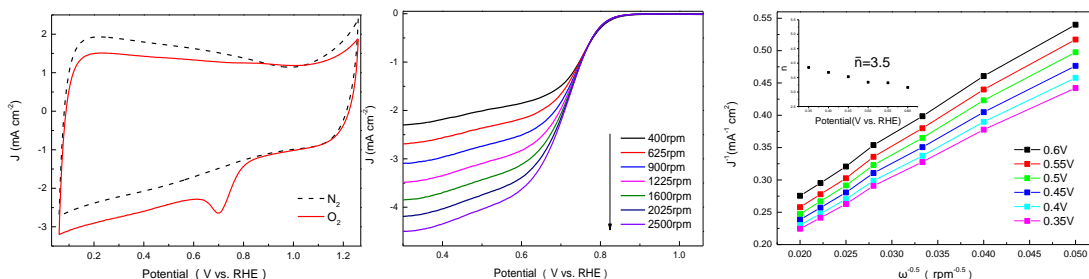
Figure S8. (A) CV curves of CSs-16h-900 in N_2 versus O_2 saturated 0.1 M KOH at 50 mV s^{-1}; (B) LSV curves of CSs-16h-900 at different rotating speeds; (C) K-L plots at different potentials.
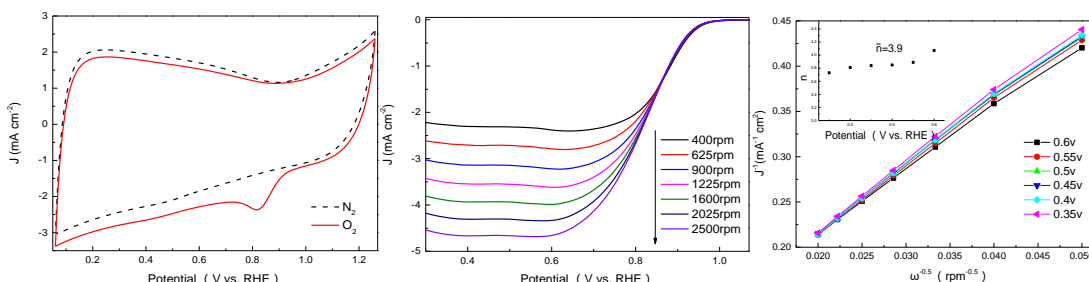

Figure S9. (A) CV curves of CSs -24h-900 in N_2 versus O_2 saturated 0.1 M KOH at 50mV s^{-1}; (B) LSV curves of CS_S -24h-900 at different rotating speeds; (C) K-L plots at different potentials.

Figure S10. (A) CV curves of CSs -28h-900 in N_2 versus O_2 saturated 0.1 M KOH at 50mV s^{-1}; (B) LSV curves of CS_S -28h-900 at different rotating speeds; (C) K-L plots at different potentials.
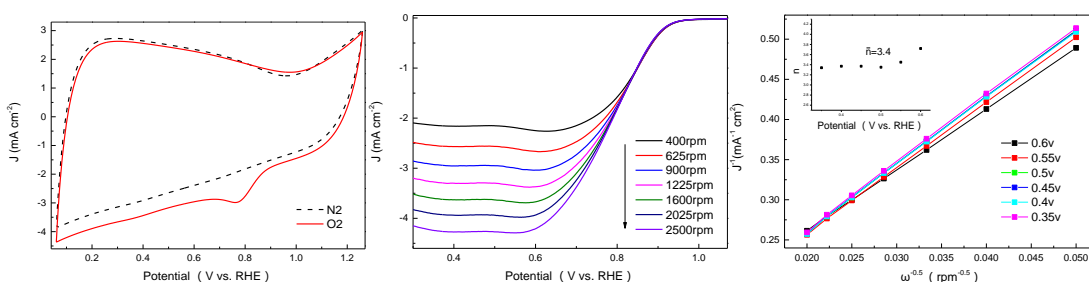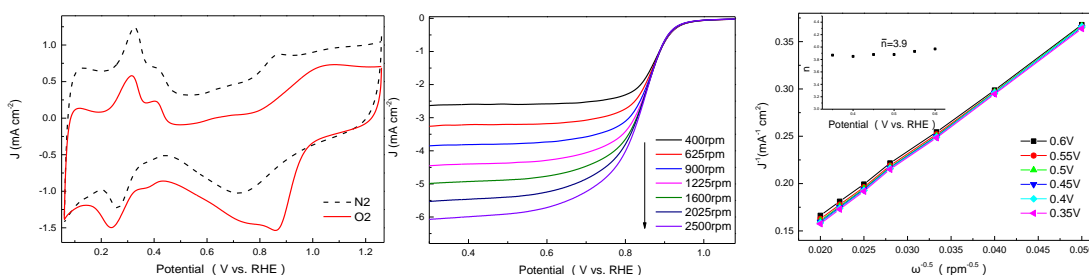

Figure S11. (A) CV curves of Pt/C in N_2 versus O_2 saturated 0.1 M KOH at 50mV s^{-1}. (B); LSV curves of Pt/C at different rotating speeds; (C) K-L plots at different potentials.

Under inert N_2 environment, the CV curves for all catalysts were quasi rectangular with no reduction peaks. In O_2-saturated 0.1 M KOH solutions, oxygen reduction peaks were observed clearly for all samples, indicating the CSs possessed significant ORR activities.

8

Table S1 Composition, specific surface area and electroactivity of all catalysts.

Samples	S_{BET} $(m^2\ g^{-1})$	I_D/I_G	E_{onset} (V)	$E_{1/2}$ (V)	J_L $(mA\ cm^{-2})$	n
CSs-16h-900	985	2.19	0.832	0.72	3.77	3.5
CSs-20h-900	756	1.81	0.979	0.835	4.17	3.9
CSs-24h-900	649	1.39	0.916	0.826	3.92	3.9
CSs-28h-900	629	1.35	0.886	0.80	3.62	3.4
Pt/C	--	--	0.962	0.855	5.15	3.9

Table S2 Comparison of the ORR activities of metal-free electrocatalysts (in 0.1 M KOH).

Catalysts	E_{onset} (V) vs.RHE	$E_{1/2}$ (V) vs.RHE	J_L $(mA\ cm^{-2})$	n	Ref.
P-Graphene	0.92	N.A.[a]	3.67	3.0~3.8	*Adv Mater* 2013, 25, 4932
N,S,O-OMC	0.85	0.75	3.8	3.5	*J Am Chem Soc* 2014, 136, 8875
Defective Carbon Nanocages (CNCs)	0.88	N.A.[a]	3.1	2.9	*ACS Catalysis* 2015, 5, 6707
Nanosheets N-CNS-120	0.896	0.757	5.79	3.9~4.0	*Adv Mater* 2016, 28, 5080
CSs-20h-900	0.98	0.84	4.2	3.9	In this work

[a] N.A.: not available.

It can be seen that these samples CSs-20h-900 outperform most previously reported metal-free carbon-based ORR catalysts

[1] X. Wang, X. Li, C. Ouyang, Z. Li, S. Dou, Z. Ma, L. Tao, J. Huo, S. Wang, *J. Mater. Chem. A* **2016**, 4, 9370.